Kinetics and Catalysis, Vol. 42, No. 4, 2001, pp. 443–451. Translated from Kinetika i Kataliz, Vol. 42, No. 4, 2001, pp. 493–502.
Original Russian Text Copyright © 2001 by Zhil'tsova, Zaslonlko, Karasevich.

Application of the Monte Carlo Method to Modeling Kinetic Processes of Polyatomic Molecules and Clusters: III. Kinetics of Reversible Reactions of Polyatomic Molecules

I. V. Zhil'tsova, I. S. Zaslonlko[†], and Yu. K. Karasevich

Semenov Institute of Chemical Physics, Russian Academy of Sciences, Moscow, 177977 Russia

Received December 4, 2000

Abstract—The Monte Carlo simulations of the reversible isomerization is carried out. The rate constants for the forward and reverse reaction of dichloroethylene *cis*–trans isomerization are determined for a broad range of initial conditions. Its is shown that the mutual effect of two actively interacting reactions occurring with energy exchange leads to a number of kinetic features of the process: characteristic changes in the rate constants during the process and the dependence of the equilibrium values of rate constants on pressure. The physical nature of these features associated with the disturbance of the function of distribution over vibrational energy due to the reaction is discussed.

INTRODUCTION

This work continues a series of our publications [1–4] devoted to statistical Monte Carlo (MC) modeling of the kinetics of physicochemical processes with the participation of polyatomic molecules and clusters. The idea of the method consists in the computational imitation of physicochemical processes in gases, including energy exchange during collisions of molecules and clusters with diluent gas species, chemical reactions, and electron and light emission. To determine the probability of different processes using this method, we used the models of energy exchange and reactions based on the statistical theory of unimolecular reactions. For instance, the MC method was used to model the processes of energy exchange and reactions of polyatomic molecules in the framework of the model of activation via the formation of the statistical collisional complex [1, 2]. We also applied the MC methods to the modeling of the emission processes in metal clusters (cluster decomposition, ionization, and radiation) under the conditions far from equilibrium to describe energy exchange between clusters and surrounding gas molecules using the step-ladder model [3, 4]. The basis for determining kinetic characteristics of processes is the nonequilibrium function of molecule and cluster distribution over energy. This function was constructed by the play-off of many random events. The distribution function was used to calculate the rate constants, emission spectra, etc. This article deals with further development of the method of statistical modeling as applied to the reversible isomerization reactions of polyatomic molecules.

CALCULATION PROCEDURE

The *cis*–*trans* isomerization of dichloroethylene was used as a model reaction:

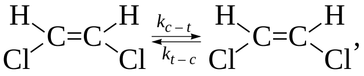

$$\mathrm{(H)(Cl)C{=}C(H)(Cl)} \underset{k_{t-c}}{\overset{k_{c-t}}{\rightleftarrows}} \mathrm{(H)(Cl)C{=}C(Cl)(H)}, \qquad \text{(I)}$$

where k_{c-t} and k_{t-c} are the rate constants of *cis*–*trans* and *trans*–*cis* isomerizations, respectively (henceforth, the former reaction will be considered the forward direction and the latter will be considered as reverse). Figure 1 shows the scheme of the potential energy surface for this reaction. Analysis of the kinetics of reaction (I) at low pressures was carried out in [5] by solving the set of differential equations for the populations of energy states. The solutions were used to calculate the macroscopic rate constants of the forward and reverse isomerization reactions of the model molecule and changes in the concentrations of each isomer in time. This fact makes it possible to compare the results obtained by different methods. In this work, calculations were carried out for high temperatures (1750–2500 K) for the reasons considered below. Under these conditions, in addition to isomerization, dichloroethylene decomposition may occur, but we excluded this reaction from consideration because our goal here is to demonstrate the capabilities of the MC method as applied to reversible reactions. This is why the dichloroethylene should be considered as a model molecule. Note that there are no principle constraints for considering isomerization and dissociation together using the MC method.

To carry out MC simulations, it is necessary to define the functions of the density of vibrational states for each isomer $\rho_c(E)$ and $\rho_t(E)$ (henceforth, the subscript "*c*" refers to the *cis*-isomer and the subscript "*t*"

[†] Deceased.

0023-1584/01/4204-0443$25.00 © 2001 MAIK "Nauka / Interperiodica"

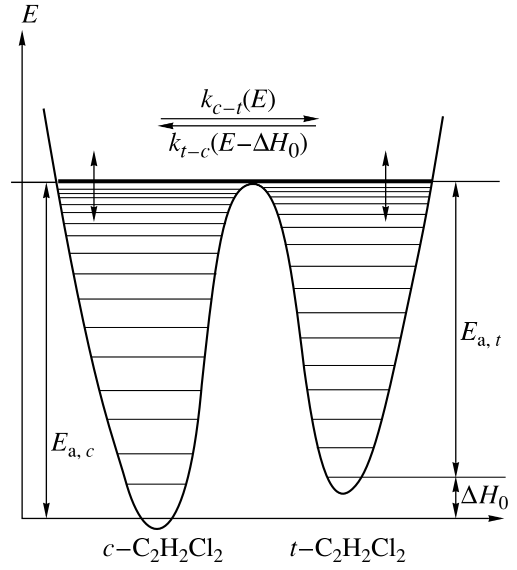

Fig. 1. Diagram of the potential energy surface for the *cis–trans* isomerization of dichloroethylene. The arrows show transition to the field of active states.

refers to the *trans*-isomer), specific rate constants for the forward $k_{c-t}(E)$ and reverse $k_{t-c}(E)$ reactions. The functions of the density of vibrational states were calculated using the procedure described in [2], which makes it possible to obtain the approximation formulas in the following form:

$$\rho(E) = \frac{s}{E_0}\left(1+\frac{E}{E_0}\right)^{s-1},$$

where s is the effective statistical weight of vibrational states; E_0 is the approximation parameter, which means the effective energy of zero-point vibrations of a molecule; E is the energy calculated with reference to the zero-point vibration energy. The following characteristic vibration frequencies of *cis*- and *trans*-dichloroethylene were taken for calculations [6]:

cis-$C_2H_2Cl_2$: 3077, 3072, 1587, 1294, 1179, 848, 711, 571, 173, 876, 406, and 679 cm^{-1} and

trans-$C_2H_2Cl_2$: 3073, 3080, 1578, 1274, 1200, 846, 817, 350, 250, 895, 227, and 763 cm^{-1}.

As a result, we obtained for *cis*-$C_2H_2Cl_2$ $s_c = 10.404$ and $E_{0,c} = 37.47$ kJ/mol and for *trans*-$C_2H_2Cl_2$: $s_t = 10.315$, and $E_{0,t} = 35.47$ kJ/mol.

The specific rate constants $k_{c-t}(E)$ and $k_{t-c}(E)$ were determined using experimental data on macroscopic rate constants of the forward and reverse reactions (I) in the high-pressure limit [7–9]. In this work we also used data from [8], where the rate constants for both reactions were determined experimentally:

$$k_{c-t}(T) = 5.7\times10^{12}\exp(-234.3/RT),$$

$$k_{t-c}(T) = 4.8\times10^{12}\exp(-231.4/RT)$$

where the activation energy is in kJ/mol.

Taking these data into account, the specific rate constants are

$$k_{c-t}(E) = 5.7\times10^{12}\left(1-\frac{E_c}{E-E_{0c}}\right)^{s_c-1},$$

$$k_{t-c}(E) = 4.8\times10^{12}\left(1-\frac{E_t}{E-E_{0t}}\right)^{s_t-1},$$

where $E_c = 234.3$ kJ/mol and $E_t = 231.4$ kJ/mol are the energy barriers for the forward and reverse reactions, respectively.

The main procedures in the MC modeling of energy exchange and dissociation of polyatomic molecules were described in detail in [1, 2]. The calculation procedure in the case of reversible isomerization is basically the same, but some differences can also be mentioned. In the latter case it is necessary to consider the transformations of the function of distribution over energy for each isomer at the same time.

At the first stage, N molecules (usually $N \sim 10^6$) were placed along the scale of full energies of molecules in the cells with sizes of $\sim RT/10$ according to the arbitrary initial distribution function. The value of N was chosen to compromise between time expenses for calculation and its accuracy as considered below. The initial distribution function was either the equilibrium function under given condition or the equilibrium function at a temperature other than the temperature of the diluent gas. The letter was used to describe the kinetics that accounts for the relaxation of the distribution function. In most cases we considered the situation when only one isomer was present in the initial mixture, but in some cases we also considered both isomers at a certain ratio.

We assumed that all molecules collide and change their energy states together in periods of time, which were all equal to the average time of between their collisions with diluent gas molecules. Reactions were assumed to occur between collisions. For convenience of further discussion, we will refer to collisions of isomeric molecules with the molecules of a diluent gas and isomerizations reactions as *events*. We will call a *cycle* the procedure consisting of the play-off of events for all N molecules. Play-off was carried out as follows. The full energy of a molecule E_Σ was distributed between vibrational E_v and rotational E_r components. The procedure of distributing the energy was described in detail in [1, 2]. If the vibrational energy of a molecule was below the reaction barrier, we considered that the molecule was not isomerized between collisions. In this case, we played off the collision and determined the new energy state of the molecule. If the value of E_v was higher than the reaction barrier, then we determined the isomeric state of a molecule, played off a collision for the determined isomer, and then determined its new energy state.

The latter element of the calculation procedure requires further explanation. Let us consider in more detail how isomerization occurs. If one isomeric molecule (e.g., *cis*-isomer) appears at the state with vibrational energy higher than the reaction barrier in the course of random traveling, then there is some probability that it will transform into the *trans*-isomer. This probability is determined by the value of the specific rate constant $k_{c-t}(E)$. However, the *trans*-isomer molecule formed by the reaction is also above the reaction barrier and can transform back to the *cis*-isomer with the rate constant $k_{t-c}(E - H_0)$ (see Fig. 1). Thus, for the time between two collisions, multiple isomerizations may occur. It is easy to show that the probabilities that the *cis*-isomer will appear at the *trans* state and the *trans*-isomer will appear at the *cis* state are equal to

$$p_{c-t}(E) = \frac{k_{c-t}(E)}{k_{c-t}(E) + k_{t-c}(E - \Delta H_0)} \times \left[1 - \exp\left(-\frac{k_{c-t}(E) + k_{t-c}(E - \Delta H_0)}{Z}\right)\right],$$

$$p_{t-c}(E) = \frac{k_{t-c}(E)}{k_{t-c}(E) + k_{c-t}(E + \Delta H_0)} \times \left[1 - \exp\left(-\frac{k_{t-c}(E) + k_{c-t}(E + \Delta H_0)}{Z}\right)\right],$$

respectively, where $Z = 2.7 \times 10^{11}\, PT^{-1/2}$ s^{-1} is the frequency of molecule collisions with the medium species (P is the gas pressure). Therefore, to determine the state of the *cis*-isomer with energy higher than the reaction barrier by the instant of the next collision, we played off the random number $\xi \in [0, 1]$. If $\xi < p_{c-t}(E)$, we considered that the isomerization occurred and increased the value ΔN_{c-t} of a counter for the *cis–trans* isomerization. Otherwise, we considered that the molecule preserved its isomeric configuration. In a similar manner, we considered the probability of the backward reaction.

After carrying out one-cycle calculations for each isomer, we determined the numbers of molecules that isomerized into a different configuration ΔN_{c-t} and ΔN_{t-c} for the period between two consecutive collisions. We also determined the distribution function for both isomers formed by the end of a cycle. These data were a source for determining the values of the relative concentrations of isomers and for determining the macroscopic rate constants in each cycle. A series of several cycles gave us the kinetic pattern of the behavior up to establishing the equilibrium between isomers.

The macroscopic rate constants for reversible isomerization $k^{(1)}(T)$ and $k^{(2)}(T)$ were determined using two methods. The results depended substantially on the method. The first method consisted in determining the changes in the relative concentrations of each isomer for an elementary period of time (in our case the period between two consecutive collisions). Then, for the rate constants, we had

$$k^{(1)}_{c-t}(T) = Z\frac{\Delta H_{c-t}}{N_c}, \quad k^{(1)}_{t-c}(T) = Z\frac{\Delta H_{t-c}}{N_t}, \tag{1}$$

where N_c and N_t are the initial numbers of *cis*- and *trans*- isomers at the initial moment of the cycle. The second method employed the following formulas of the statistical theory of unimolecular reactions [10]

$$\begin{aligned} k^{(2)}_{c-t}(T) &= \int_{E_c}^{\infty} k_{c-t}(E)F_{\mathrm{v},c}(E)dE, \\ k^{(2)}_{t-c}(T) &= \int_{E_c}^{\infty} k_{t-c}(E)F_{\mathrm{v},t}(E)dE, \end{aligned} \tag{2}$$

where $F_{\mathrm{v},c}(E)$ and $F_{\mathrm{v},t}(E)$ are the functions of distribution over the vibrational energy for *cis*- and *trans*-isomers, respectively.

The error in determining the number of isomerized molecules in a cycle and in determining the isomerization rate constants was estimated by the formula

$$\delta = \frac{\mathrm{d}(\Delta N)}{\Delta N} = \frac{dk(T)}{k(T)} \approx \sqrt{\frac{Z}{Nk(T)}}. \tag{3}$$

Therefore, we see that an error increases with an increase in the frequency of vibrations or pressure and with a decrease in the rate constant (i.e., with a decrease in temperature). Provided that the error should not be higher than 20%, we used this formula to determine the region of conditions under which the application of the method gives optimal results. The number N of dichloroethylene molecules was varied in the interval $(0.5–2) \times 10^6$ and was determined by time one could spend on computation. Note that, to obtain one kinetic curve, it was necessary to calculate hundreds and sometimes thousands of cycles, and the time required for the average one-cycle calculation was ~1.5 min for 166-MHz PC used in this work. The range of pressures in our calculation was 0.001–10 atm. This range was the most interesting from the standpoint of experimental studies. Under these conditions, the temperature interval optimal for calculation was 1750–2500 K.

RESULTS OF CALCULATION

The determining factor for the kinetics of reversible isomerization is the state of the function of isomer distribution over vibrational energy and their transformation during the process. When the mixture of composition is nonequilibrium, the typical state of the distribution function for both isomers takes the form shown in Fig. 2. The distribution functions shown in this figure correspond to the moment when the mixture contained 90% *cis*- and 10% *trans*-isomer (in the equilibrium, the concentrations of both forms are about the same). It is

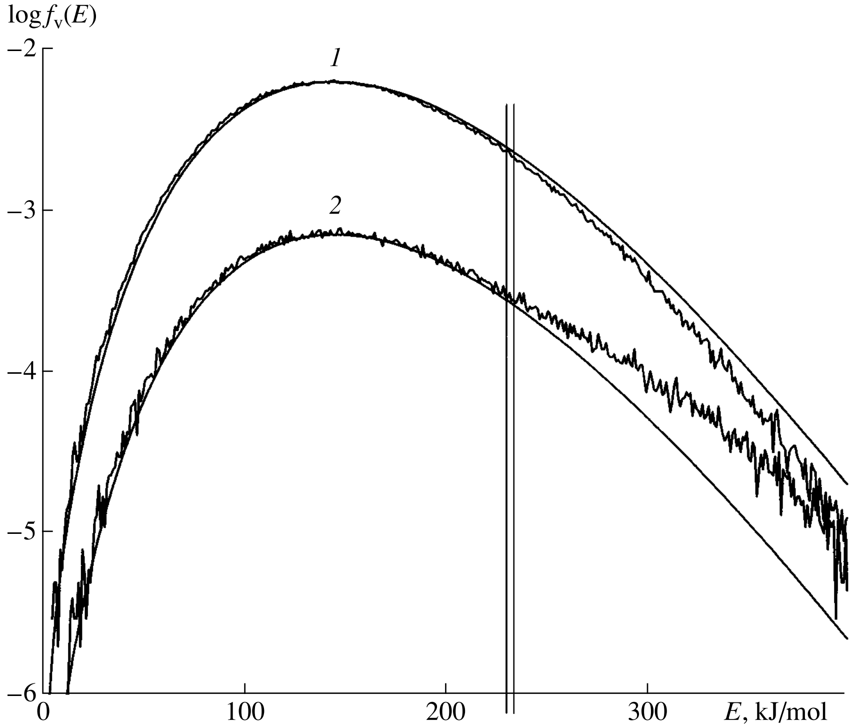

Fig. 2. Functions of the distribution over vibrational energies for (*1*) *cis* and (*2*) *trans*-$C_2H_2Cl_2$ at an nonequilibrium composition of the mixture (90% *cis* and 10% *trans*) at 2000 K and 0.1 atm. Smooth lines show equilibrium distribution functions.

clearly seen that above the reaction barrier E_d, the distribution function for the *cis*-isomer is depleted, and that for the *trans*-isomer is enriched compared to the equilibrium distribution functions shown in Fig. 2 with smooth curves. The nonequilibrium state of the distribution functions of isomers substantially affects the values of isomerization rate constants and the dependences of isomer concentration changes on time.

Figure 3 shows changes in the isomer concentrations on time expressed in the number of collisions. The calculation was carried out for an initial state when only *cis*-isomer was present in the mixture to the achievement and up to attaining the equilibrium composition at T = 2000 K and P = 0.1 atm. At the initial portion of kinetic curves, we observed a short induction period that lasted 25–30 collisions. This was due to the relaxation of the vibrational temperature of dichloroethylene from 300 K to 2000 K that imitated a jumpwise change in the conditions behind the front of the shock wave. Problems associated with the relaxation of vibration temperature were considered in detail in [1, 2].

The specific features of the reversible isomerization due to nonequilibrium conditions are clearly seen in the changes of rate constants in the course of the process. Figure 4 shows the plots of $k^{(1)}_{c-t}$ and $k^{(1)}_{t-c}$ vs. time expressed in terms of the number of collisions. These were constructed using Eq. (1) for 2500 K and 0.001 atm for the case when the initial mixture contains only one isomer. Figure 4 shows the results of two calculations when the distribution function of the reactive species corresponds to 300 K (curves *1* and *2*) and 2500 K (curves *3* and *4*). In the case of low-temperature initial distribution function, after a short induction period of temperature relaxation, the rate constant of the forward reaction starts to increase and gradually reaches the equilibrium value. The rate constant increases in jumpwise manner, reaches very high values, and then gradually decreases to the equilibrium value. When the initial distribution function already corresponds to the temperature of the buffer gas, the rate constant of the forward reaction initially has the equilibrium value, and then somewhat decreases. After reaching a minimum, it starts to increase tending to the equilibrium value. The behavior of the rate constant of the reverse reaction is qualitatively the same as in the case of low-temperature initial distribution function, but the value of the initial jump is substantially lower.

If we define the rate constants of isomerization using Eq. (2), then changes in $k^{(2)}_{c-t}$ and $k^{(2)}_{t-c}$ in the course of the reaction are similar to constants (1), but the absolute values of $k^{(2)}_{c-t}$ and $k^{(2)}_{t-c}$ are higher than $k^{(1)}_{c-t}$ and $k^{(1)}_{t-c}$ during the whole process and remain high after the equilibrium composition of the mixture is reached. Figure 5 illustrates this; it shows both changes in the constants $k^{(1)}_{c-t}$ and $k^{(1)}_{t-c}$ (curves *1*, *1*', *2*, and *2*') and $k^{(2)}_{c-t}$, and $k^{(2)}_{t-c}$ (curves *3*, *3*', *4*, and *4*') depending on the relative fraction of the *cis*-isomer in the mixture. Calculations of two types were carried out. In the first of them, only the *cis*-isomer was present at the initial moment (the right side of the figure) and in the second case only the *trans*-isomer was present (the left side). In both cases, the calculation was carried out until the equilibrium composition of the mixture was achieved (the equilibrium state is shown in the figure with a vertical line). A series of similar calculations showed that the difference between the rate constants determined by Eqs. (2) and (1) increases with a decrease in pressure.

Figures 4 and 5 show how the error in determining the isomerization rate constants changes. At 2000 K and 0.1 atm (Fig. 5) the scatter of the calculated constants is substantial, whereas it is almost unnoticeable at 2500 K and 0.01 atm (Fig. 4). Formula (3) predicts that the error increases with a decrease in temperature or with an increase in pressure. This fact constrains the region where the MC method is applicable.

Figure 6 shows the dependence of the rate constant $k^{(1)}_{c-t}$ (solid lines) and $k^{(2)}_{c-t}$ (horizontal segments of straight lines) on pressure for the forward reaction at an equilibrium state of the reaction mixture composition. It is seen that the constant determined by Eq. (2) is independent of pressure and the constant determined by Eq. (1) leads to a decrease in pressure to its minimal value achieved in the high-pressure limit and is proportional to pressure in the low-pressure limit. Figure 7 shows the temperature dependences of the same constants at different pressures. The higher the pressure (curves *1*–*5*), the higher the values of $k^{(1)}_{c-t}$. In the high-pressure limit they correspond to the dependence of the pressure-independent constants $k^{(2)}_{c-t}$ (dashed lines) on temperature. The temperature dependence of $k^{(2)}_{c-t}$ in turn coincides with the experimental dependence in the high-pressure limit [8].

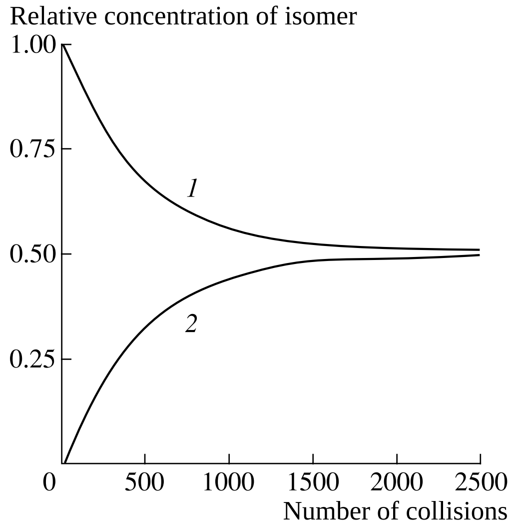

Fig. 3. Dependence of the relative concentrations of (*1*) *cis* and (*2*) *trans*-isomers on time (expressed in the number of collisions) at 2000 K and 0.1 atm and the initial distribution function corresponding to 300 K. The initial mixture contained only the *cis*-isomer.

DISCUSSION

The reversible unimolecular reaction has several specific features, which were observed when we considered the results of MC modeling. First, these are the characteristic changes in the rate constants in the course of reaction. Second, this is the dependence of the equilibrium values of rate constants on pressure. Let us analyze the main regularities of isomerization kinetics using the Lindemann scheme [11] modified for the description of the reversible reaction [5]:

$$1)\ \ A + M \underset{k_{-1}}{\overset{k_1}{\rightleftarrows}} A^* + M,$$

$$2)\ \ A^* \underset{k_{BA}}{\overset{k_{AB}}{\rightleftarrows}} B^*, \qquad (II)$$

$$3)\ \ B^* + M \underset{k_3}{\overset{k_{-3}}{\rightleftarrows}} B + M.$$

Steps (1) and (3) are the reversible processes of isomers A and B activation and deactivation in collisions with species M of the medium. Step (2) reflects interconversions of the active states of isomers A* and B*.

For the sake of simplicity, we will consider that both isomers have the same dynamic characteristics (this is a correct assumption for the model molecule). That is, we assume that $k_1 = k_3$, $k_{-1} = k_{-3}$, and $k_{AB} = k_{BA}$. Using these assumptions we obtain for the relative concentrations X_{A*} and X_{B*} of excited molecules A* and B*

$$X_{A*} = \frac{k_1}{k_1 + k_{-1}}\frac{1 + \alpha X}{2 + \alpha},$$

$$X_{B*} = \frac{k_1}{k_1 + k_{-1}}\frac{1 + \alpha(1 - X)}{2 + \alpha},$$

where $X = X_A + X_{A*}$ is the total relative concentration of the initial isomer in the active and inactive, $\alpha = (k_1 + k_{-1})C_M/k_{AB}$, and C_M is the concentration of the molecules of buffer gas. The rate of isomer A transformation is

$$w_{AB} = k_{AB}X_{A*}. \qquad (4)$$

Therefore, we obtain for the apparent rate constant determined as a specific rate of isomerization

$$k^{(I)}_{\text{эф},\,AB} = \frac{w_{AB}}{x} = \frac{k_{AB}k_{-1}}{k_1 + k_{-1}}\frac{1 + \alpha X}{(2 + \alpha)X}. \qquad (5)$$

Analogously, we obtain for the reverse reaction

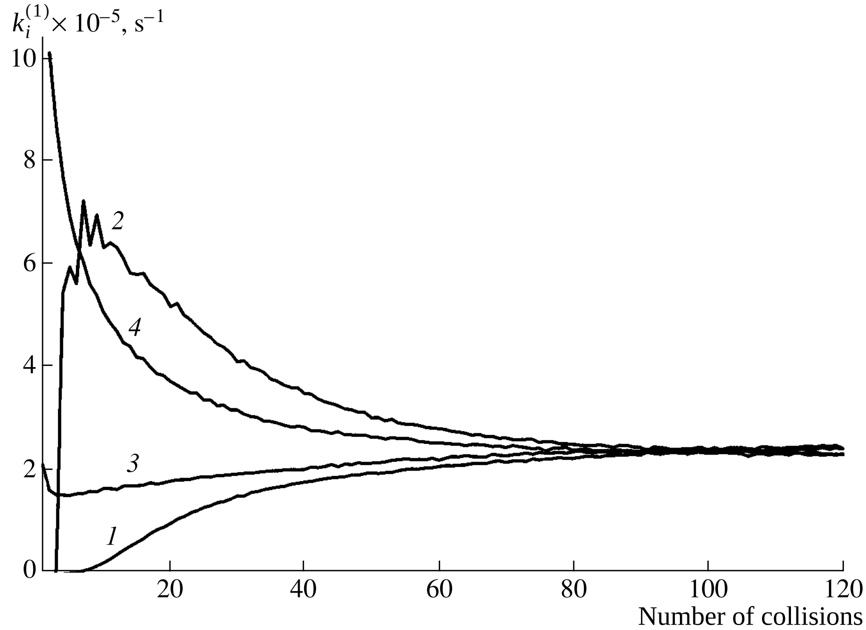

Fig. 4. Dependences of the rate constants ($k_i^{(1)}$) of reversible isomerization on time (expressed in the number of collisions) at 2500 K and 0.01 atm and the initial distribution function corresponding to 300 K (*1*) $k_{c-t}^{(1)}$ and (*2*) $k_{t-c}^{(1)}$ and 2500 K (*3*) $k_{c-t}^{(1)}$ and (*4*) $k_{t-c}^{(1)}$. At the initial moment the system contained *cis*-isomer.

$$k^{(\mathrm{I})}_{\mathrm{app,\,BA}} = \frac{w_{\mathrm{BA}}}{1-X} = \frac{k_{\mathrm{AB}}k_1}{k_1+k_{-1}}\frac{1+\alpha(1-X)}{(2+\alpha)(1-X)}. \qquad (6)$$

The expression for the rate of isomerization (4) and the corresponding constants $k^{(\mathrm{I})}_{\mathrm{app,\,AB}}$ and $k^{(\mathrm{I})}_{\mathrm{app,\,BA}}$ describe all possible acts of isomerization. However, in step (2) isomeric transformations with the participation of the active molecule between two consecutive collisions of this molecule with buffer gas species create two oppositely oriented flows that compensate for each other and do not result in the changes in the isomer concentrations. To take this into account, the factor $\frac{k_{-1}C_{\mathrm{M}}}{k_{\mathrm{AB}}+k_{-1}C_{\mathrm{M}}}$ should be introduced into Eqs. (4)–(6). In this case the expressions for the rate constants take the following forms:

$$k^{(\mathrm{I})}_{\mathrm{app,\,AB}} = \frac{k_1k_{-1}C_{\mathrm{M}}^2}{k_{\mathrm{AB}}+k_{-1}C_{\mathrm{M}}}\frac{1+\alpha X}{\alpha(2+\alpha)X}, \qquad (7)$$

$$k^{(\mathrm{I})}_{\mathrm{app,\,BA}} = \frac{k_1k_{-1}C_{\mathrm{M}}^2}{k_{\mathrm{AB}}+k_{-1}C_{\mathrm{M}}}\frac{1+\alpha(1-X)}{\alpha(2+\alpha)(1-X)}. \qquad (8)$$

The above equations show that apparent rate constants (5)–(8) depend on the concentration X of the isomer A and change in the course of reaction. The reason for such a dependence is the disturbance of the equilibrium distribution of both isomers over energy as a result of the reaction. As can be seen from scheme (II), the formation of excited molecules of each isomer occurs as a result of energy exchange in collisions and isomerization. On the one hand, the forward reaction results in a decrease in the concentration of highly excited molecules of the initial isomer. One the other hand, the forward reaction should be considered as additional chemical activation for the reverse reaction because the molecule of the product isomer is highly excited when it is formed. This excitation is preserved at least up to the moment when the product collides with the diluent gas. At the same time, the reverse reaction affects the forward reaction in a similar way. It results in populating the highly excited states of the initial molecule. Thus, up to the moment when the equilibrium composition of the reaction mixture is achieved and when the forward and reverse reactions balance each other, the concentrations of excited molecules of both isomers differ from their equilibrium values: for the initial isomer it is lower and for the product isomer it is higher than the equilibrium values (see Fig. 2). The magnitude of this effect depends on the ratio of the rates of the forward and reverse reactions and as a consequence on the ratio of isomer concentrations. The apparent rate constants of isomerization are in turn determined by the concentrations of molecules above the reaction barrier, and this results in their dependence on the ratio between the concentrations of isomers in the course of the reaction.

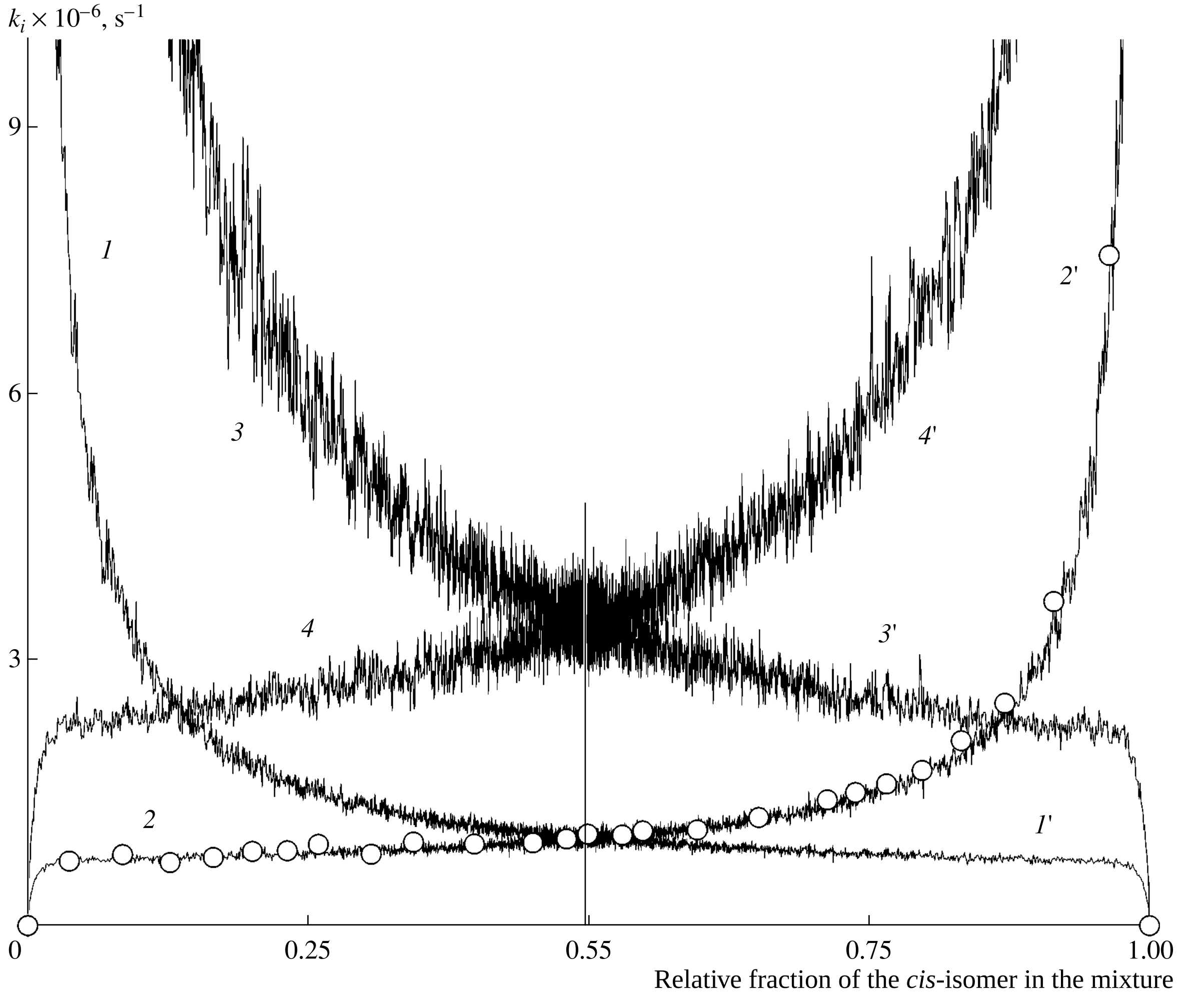

Fig. 5. Dependences of the rate constants (k_i) of the forward and reverse isomerization reactions on the relative fraction of the *cis*-isomer in the mixture at 2000 K and 0.1 atm: (*1*, *1*') $k^{(1)}_{c-t}$, (*2*, *2*') $k^{(1)}_{t-c}$, (*3*, *3*') $k^{(2)}_{c-t}$, and (*4*, *4*') $k^{(2)}_{t-c}$. (*1*–*4*) Calculation from the initial mixture contains only the *trans*-isomer to the equilibrium composition. Open circles shows the calculation of the $k^{(1)}_{t-c}$ values using the $k^{(1)}_{c-t}$ values and formula (12).

The rate with which the total relative concentration of the initial isomer X changes can be described in the following form:

$$\frac{\mathrm{d}X}{\mathrm{d}t} = \frac{\mathrm{d}X_{\mathrm{A}}}{\mathrm{d}t} + \frac{\mathrm{d}X_{\mathrm{A}^*}}{\mathrm{d}t} = -k_{\mathrm{AB}}(X_{\mathrm{A}^*} - X_{\mathrm{B}^*})$$
$$= -\frac{k_1 C_{\mathrm{M}}}{2+\alpha}[X - (1 - X)].$$

This expression functionally coincides with the expression for the rate of changing the relative concentration of the initial isomer in the one-step reaction A $\rightleftarrows$ B when the forward and reverse rate constants are the same:

$$k^{(\mathrm{III})}_{\mathrm{app,\,AB}} = k^{(\mathrm{III})}_{\mathrm{app,\,BA}} = \frac{k_1 C_{\mathrm{M}}}{2+\alpha} \qquad (9)$$

This expression suggests that although the nonequilibrium distribution of isomers over energies during the reaction is a characteristic feature of the process, the disturbance in the distribution function for reacting molecules is such that the macrokinetic changes in the concentrations of both isomers follow the simple mass action law. The rate constants in this case are the combinations of the rate constants of separate steps of the process.

After analyzing kinetic scheme (II), we obtained three different pairs of expressions for the apparent rate constants of the forward and reverse isomerization reactions. Each of these pairs allows one to calculate the macrokinetic profile of changes in the concentrations of isomers, but the physical meaning of these constants and their properties are different. The constants

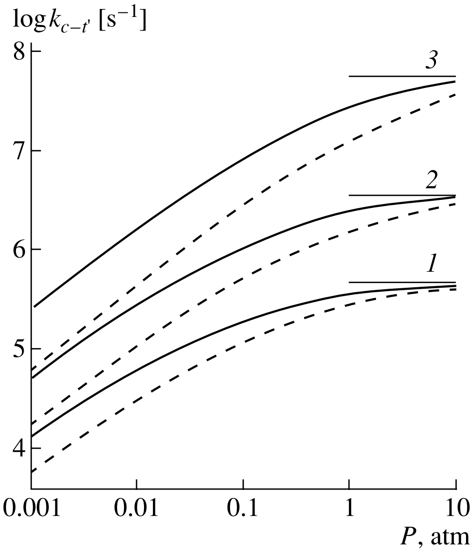

Fig. 6. Dependences of the rate constants of the transition from the *cis*- to *trans* states of $C_2H_2Cl_2$ k_{c-t} on pressure at temperatures (*1*) 1750 K, (*2*) 2000 K, and (*3*) 2500 K. Horizontal segments show $k_{c-t}^{(2)}$, solid lines show $k_{c-t}^{(1)}$, and dashed lines show $k_{c-t}^{(3)}$.

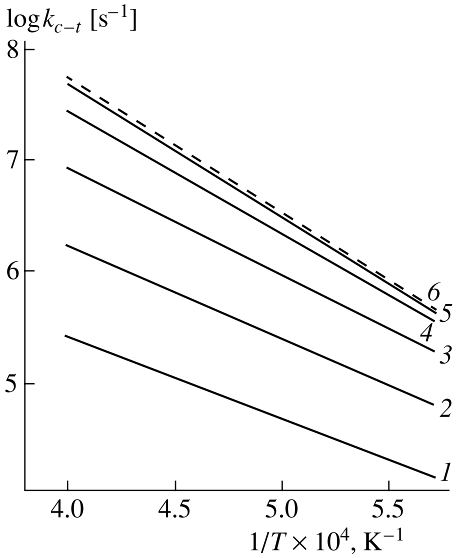

Fig. 7. Dependences of the rate constants of the transition from the *cis*- to *trans* states of $C_2H_2Cl_2$ on temperature: (*1*–*5*) calculation using formula (1) at (*1*) 0.001, (*2*) 0.01, (*3*) 0.1, (*4*) 1 and (*5*) 10 atm; (*6*) calculation using formula (2) at any pressure and the coinciding experimental dependence [8] in the high-pressure limit.

$k_{\mathrm{app,\,AB}}^{(\mathrm{I})}$ and $k_{\mathrm{app,\,BA}}^{(\mathrm{I})}$ obtained from Eqs. (5) and (6) determine the complete rate of isomeric transformations, whereas $k_{\mathrm{app,\,AB}}^{(\mathrm{II})}$ and $k_{\mathrm{app,\,BA}}^{(\mathrm{II})}$ obtained from Eqs. (7) and (8) determine only a component of the complete rate that results in changes in the concentrations of isomers. The rate constants $k_{\mathrm{app,\,AB}}^{(\mathrm{III})}$ and $k_{\mathrm{app,\,BA}}^{(\mathrm{III})}$ in Eq. (9) result from mathematical rearrangements that reduce the representation of multistep kinetics to the form of the kinetics of one-step reversible reaction.

All three pairs of rate constants respond to the changes in the pressure in a different manner. Let us first consider the dependences of rate constants on pressure taken under the conditions of material and energy equilibrium. Assuming the same dynamic characteristics of isomers, the ratio of their concentrations at equilibrium is equal to unity 1 ($X = 1/2$) and the rate constants of the forward and reverse processes are equal. In the high-pressure (hp) limit ($\alpha \longrightarrow \infty$), all three types of constants coincide:

$$k_{\mathrm{app}}^{\mathrm{hp}} = \frac{k_1 k_{\mathrm{AB}}}{k_1 + k_{-1}}.$$

With a decrease in pressure, the rate constants determined by Eqs. (5) and (6) do not change. The constants determined by Eqs. (7)–(9) depend on pressure. For the process under study, this dependence is due to the necessity of collisional stabilization of excited reacting molecules for transforming one isomer into another. In the low-pressure (lp) limit ($\alpha \longrightarrow 0$), these constants become proportional to the pressure of buffer gas:

$$k_{\mathrm{app}}^{(\mathrm{II,\,lp})} = \frac{k_1 k_{-1} C_{\mathrm{M}}}{k_1 + k_{-1}}, \tag{10}$$

$$k_{\mathrm{app}}^{(\mathrm{III,\,lp})} = 1/2 k_1 C_{\mathrm{M}}. \tag{11}$$

Comparison of Eqs. (10) and (11) shows that the values of rate constants determined from Eq. (9) are lower than the values determined from Eqs. (7) and (8) on the plot of their dependence on pressure (if the rate of deactivation is much higher than the rate of activation ($k_{-1} \gg k_1$), then their ratio is 1/2). The reason for a more pronounced dependence of $k^{(\mathrm{III})}$ (Eq. 9) on pressure is an additional effect associated with the above-discussed disturbance of the equilibrium functions of isomer distribution over energies in the course of the process. This results in an increase in the characteristic time of establishing the equilibrium and lowering the values of $k^{(\mathrm{III})}$.

The results of MC simulations support analytical conclusions drawn above. Thus, the rate constants $k_{c-t}^{(2)}$ and $k_{t-c}^{(2)}$ calculated using formulas (2) by the numerical integration of the distribution function found by the MC method correspond to the constants $k_{\mathrm{app,\,AB}}^{(\mathrm{I})}$ and $k_{\mathrm{app,\,BA}}^{(\mathrm{I})}$, and the constants $k_{c-t}^{(1)}$ and $k_{t-c}^{(1)}$ calculated using macrokinetic definition (1) correspond to the constants $k_{\mathrm{app,\,AB}}^{(\mathrm{II})}$ and $k_{\mathrm{app,\,BA}}^{(\mathrm{II})}$ (Eqs. (7) and (8)). The constants described by dashed curves in Fig. 6 are analogous to rate constants $k^{(\mathrm{III})}_{\mathrm{app,\,AB}}$ and $k^{(\mathrm{III})}_{\mathrm{app,\,BA}}$ (Eq. (9)). These constants were obtained by the processing of the calculated dependences of isomer concentrations on time using the method that is usually used to determine the rate constants of reversible reactions from experimental data (i.e., using the slope of the line in the $\{\ln(X - X_\infty),\ t\}$ coordinates). The functional dependences of the respective analytical expressions and the results of numerical calculation agree very well. To illustrate this, Figure 5 shows the dependence of the rate constant of the reverse reaction $k^{(1)}_{t-c}$ on time calculated using the MC method (curves *1* and *1'*) and the same dependence (open circles) calculated by multiplying the values of the rate constant of the forward reaction $k^{(1)}_{c-t}$ by the coefficient obtained from the analysis of scheme (II):

$$\beta = \frac{k_{\mathrm{app,\,BA}}}{k_{\mathrm{app,\,AB}}} = \frac{X}{1-X}\frac{1+\alpha(1-X)}{1+\alpha X}. \qquad (12)$$

To estimate the parameter α, we assumed that $k_1 \ll k_{-1}$, and the deactivation of excited molecules occurs at each collision. For k_{AB}, we used the value of the specific rate constant $k_{c-t}(\bar{E})$, where $\bar{E} \approx E_{\mathrm{a},\,c} + \nu_c RT/2$ is the average energy at which the reaction occurs, and ν_{c} is the number of vibrational degrees of freedom. Using these assumption we obtained for the case shown in Fig. 5 ($T = 2000$ K and $P = 0.1$ atm) that $\alpha = 1.73$.

To conclude the above analysis, we wish to underline that the presence of three pairs of apparent rate constants that describe the same process is due to the fact that we consider actively interacting reactions with exchange in energy and species rather than two independent reactions. Note also that all apparent constants considered above are not the rate constants in the strict sense, although they are specific reaction rates.

For practical purposes, when one considers isomerization processes and their rate laws, the most convenient form of the isomerization rate constants is Eq. (9) because in this case the constants do not change during the process unlike those defined by Eqs. (5)–(8). However, one should take into account that any other reactions of the kinetic model in which isomers are involved (e.g., the reactions of their formation by recombination or the parallel reactions of their dissociation) may substantially affect the energy states of isomers and the isomerization rate constants. This work is a good illustration of mutual effects of two reaction with the participation of the same reactants.

ACKNOWLEDGMENTS

This work was supported by the Russian Foundation for Basic Research (project nos. 98-03-32157, 98-03-04118, and 99-03-32068).

REFERENCES

1. Zaslonko, I.S. and Karasevich, Yu.K., *Kinet. Katal.*, 2000, vol. 41, no. 3, p. 333.
2. Zhil'tsova, I.V., Zaslonko, I.S., and Karasevich, Yu.K., *Kinet. Katal.*, 2000, vol. 42, no. 4, p. 485.
3. Vlasov, P.A., Karasevich, Yu.K., and Smirnov, V.N., *Teplofiz. Vys. Temp.*, 1996, vol. 34, no. 5, p. 676.
4. Vlasov, P.A., Karasevich, Yu.K., and Smirnov, V.N., *Teplofiz. Vys. Temp.*, 1997, vol. 35, no. 2, p. 200.
5. Quack, M., *Ber. Bunsen-Ges. Phys. Chem.*, 1984, vol. 88, no. 1, p. 94.
6. Krasnov, K.S., Timoshnin, V.S., Danilova, T.G., and Khandozhko, S.V., *Molekulyarnye postoyannye neorganicheskikh soedinenii. Spravochnik* (A Handbook of Molecular Constants of Inorganic Compounds), Leningrad: Khimiya, 1968.
7. Manion, J.A. and Louw, R., *Rel. Trav. Chim. Pays-Bas*, 1989, vol. 108, no. 2, p. 235.
8. Hawton, L.D. and Semeluk, G.P., *Can. J. Chem.*, 1966, vol. 44, p. 2143.
9. Jeffers, P.M., *J. Phys. Chem.*, 1974, vol. 78, p. 1469.
10. Kuznetsov, N.M., *Kinetika monomolekulyarnykh reaktsii* (Kinetics of Unimolecular Reactions), Moscow: Nauka, 1982.
11. Lindemann, F.A., *Trans. Faraday Soc.*, 1922, vol. 17, p. 598.